

Emergence of heavy tails in homogenized stochastic gradient descent

ZHE JIAO¹ AND MARTIN KELLER-RESSEL²

¹*School of Mathematics and Statistics, Northwestern Polytechnical University, Xi'an, China*

²*Department of Mathematics, TU Dresden, Germany*

²*ScaDS.ai Center for scalable data analytics and artificial intelligence, Leipzig/Dresden, Germany*

February 5, 2024

Abstract

It has repeatedly been observed that loss minimization by stochastic gradient descent leads to heavy-tailed distributions of neural network parameters. Here, we analyze a continuous diffusion approximation of SGD, called homogenized stochastic gradient descent, show that it behaves asymptotically heavy-tailed, and give explicit upper and lower bounds on its tail-index. We validate these bounds in numerical experiments and show that they are typically close approximations to the empirical tail-index of SGD iterates. In addition, their explicit form enables us to quantify the interplay between optimization parameters and the tail-index. Doing so, we contribute to the ongoing discussion on links between heavy tails and the generalization performance of neural networks as well as the ability of SGD to avoid suboptimal local minima.

1 Introduction

Stochastic gradient descent (SGD) is the cornerstone of optimization in modern deep learning (cf. Bottou et al. [2018]). In contrast to deterministic methods, it introduces stochasticity to the optimization procedure and therefore has to be analyzed from a probabilistic viewpoint. For instance, it has been observed by Martin and Mahoney [2019], Simsekli et al. [2019], Hodgkinson and Mahoney [2021], Gurbuzbalaban et al. [2021] and others, that the distributions of neural network parameters under loss minimization by SGD are typically *heavy-tailed*. This heavy-tailed behavior has been linked to the generalization performance of neural networks: Simsekli et al. [2019] give evidence that the extreme realizations of heavy-tailed random variables allow SGD to escape local minima of the loss landscape, and Hodgkinson and Mahoney [2021] argue for a negative correlation between the parameter distributions's tail-index¹ and the network's generalization performance. For these reasons, it is important to understand

the origin and effects of heavy-tailed behavior of neural network parameters in SGD. An important step in this direction has been taken in Gurbuzbalaban et al. [2021], where the tail behavior of SGD iterates is characterized in dependence on optimization parameters, dimension and Hessian curvature at the loss minimum. One limitation of Gurbuzbalaban et al. [2021] is that this link is described only qualitatively, but not quantitatively. Here, we provide an alternative approach through analyzing homogenized stochastic gradient descent, a diffusion approximation of SGD introduced in Paquette et al. [2022b], Mori et al. [2022]. Leveraging Itô calculus for diffusion processes, we are able to provide more precise bounds and estimates of the tail behavior of SGD iterates, which we subsequently validate in numerical experiments.

1.1 Our contribution

Our contribution to the analysis of heavy-tailed phenomena in SGD can be summarized as follows:

- We introduce a new method, namely comparison results in *convex stochastic order* for homogenized stochastic gradient descent. These comparison results, derived in Section 3 allow us to link SGD to the well-studied class of *Pearson Diffusions* (cf. Forman and Sørensen [2008]) and then to obtain bounds for their tail-index.
- Contrary to Gurbuzbalaban et al. [2021], who describe the tail-index only implicitly (observing phase-transitions between different regimes) our tail-index bounds are fully explicit. Moreover, their explicit form is validated in numerical experiments in Section 4.
- Our results suggest (skew) t-distributions as surrogate for parameter distributions in neural networks under SGD, in contrast to the earlier work of [Gurbuzbalaban et al., 2021] where α -stable distributions have been suggested.
- Finally, our results strongly challenge the claim that the *observed heavy-tailed behavior of SGD in practice cannot be accurately represented by an SDE driven by a*

¹The tail-index is a quantitative measure of heavy-tailedness, with a smaller tail-index indicating increased heaviness of tails; see Section 2.4.

Brownian motion’ put forward in Simsekli et al. [2020]. Our modeling approach is based on hSGD – an SDE driven by Brownian motion – which asymptotically exhibits heavy-tailed behavior with a tail-index that, in experiments, closely matches the empirical tail-index of SGD iterates on real data.

2 Background

2.1 Empirical risk minimization

The general framework for training deep neural networks is to solve the problem of empirical risk minimization (ERM)

$$\min_{x \in \mathbb{R}^d} \left\{ f(x) := \frac{1}{n} \sum_{i=1}^n f_i(x) \right\} \quad (\text{ERM})$$

where f_i denotes the loss induced by the data point $a_i \in \mathbb{R}^d$ with label/response $b_i \in \mathbb{R}$, and f is the *empirical risk* over the training data. For our theoretical and numerical analysis of heavy-tailed phenomena, as in Gurbuzbalaban et al. [2021], we assume a quadratic structure of $f_i(x)$ with the understanding that a smooth loss landscape can typically be well-approximated by a quadratic function around a local minimum. Thus, we specify the function f_i by setting

$$f_i(x) = \frac{1}{2}(a_i \cdot x - b_i)^2 + \frac{\delta}{2}\|x\|^2 := L_i(x) + \frac{\delta}{2}\|x\|^2,$$

where $L_i(x)$ is the unregularized loss on the i -th data point and $\delta \geq 0$ a regularization parameter. This is the same loss function that is used for *ridge regression* (cf. Hastie et al. [2009]). We arrange the training data into a design matrix $A \in \mathbb{R}^{n \times d}$ and label vector $b \in \mathbb{R}^n$, whose i -th row are given by a_i and b_i respectively. Thus, we have

$$f(x) = \frac{1}{2n}\|Ax - b\|^2 + \frac{\delta}{2}\|x\|^2 := \frac{1}{n}L(x) + \frac{\delta}{2}\|x\|^2$$

with gradient given by $\nabla f(x) = \frac{1}{n}\nabla L(x) + \delta x$.

2.2 Stochastic gradient descent

The standard approach to solve the problem (ERM) is to use stochastic gradient descent (SGD) or any of its generalizations involving momentum, adaptive learning rates, gradient rescaling, etc. (cf. Goodfellow et al. [2016], Bottou et al. [2018]). As a first step, we consider plain SGD with constant learning rate γ , which can be written in recursive form as

$$x_{k+1} = x_k - \gamma \nabla f_{\Omega_k}(x_k) \quad (\text{SGD})$$

where $\nabla f_{\Omega_k}(x_k) = \frac{1}{B} \sum_{i \in \Omega_k} \nabla f_i(x_k)$ and Ω_k is a batch of size $B \geq 1$ sampled uniformly and independently from $\{1, \dots, n\}$. It will be convenient to rewrite (SGD) as

$$x_{k+1} = x_k - \gamma \nabla f(x_k) + \gamma \varepsilon(x_k) \quad (1)$$

where the gradient noise is given by

$$\varepsilon(x_k) = -[\nabla f_{\Omega_k}(x_k) - \nabla f(x_k)]. \quad (2)$$

Note that the gradient noise is unbiased (i.e. $\mathbb{E}\varepsilon(x) = 0$) with covariance matrix given by²

$$\begin{aligned} C(x) &:= \mathbb{E} [\varepsilon(x)^\top \varepsilon(x)] \\ &= \frac{1}{B} \left(\frac{1}{n} \sum_{i=1}^n \nabla L_i(x)^\top \nabla L_i(x) - \frac{1}{n^2} \nabla L(x)^\top \nabla L(x) \right). \end{aligned}$$

2.3 Homogenized Stochastic Gradient Descent

Homogenized stochastic gradient descent (hSGD), introduced concurrently in Paquette et al. [2022a] and Mori et al. [2022], is a diffusion approximation of SGD described by a stochastic differential equation (SDE) driven by Brownian motion. It is obtained by matching the drift and diffusion coefficient of the SDE to the expectation and to the covariance of the gradient noise (2) and by applying the approximation (cf. Paquette et al. [2022a])

$$\begin{aligned} C(x) &\stackrel{\mathbf{I}}{\approx} \frac{1}{B} \left(\frac{1}{n} \sum_{i=1}^n \nabla L_i(x)^\top \nabla L_i(x) \right) \\ &= \frac{1}{B} \left[\frac{1}{n} \sum_{i=1}^n (a_i \cdot x - b_i)^2 a_i^\top a_i \right] \\ &\stackrel{\mathbf{II}}{\approx} \frac{2}{n^2 B} L(x) \nabla^2 L(x), \end{aligned}$$

in which

- the approximation **I** is true due to the fact that the gradient noise variance dominates the gradient mean near minima which is based on Smith and Le [2018];
- the approximation **II** comes from the decoupling approximation (cf. Mori et al. [2022]).

Note that hSGD differs from the well-known Ornstein-Uhlenbeck approximation of Mandt et al. [2016], Jastrzebski et al. [2017], which uses a deterministic approximation of the diffusion coefficient, whereas the diffusion coefficient of hSGD is stochastic. Paquette et al. [2022a] show both analytically and in experiments that hSGD approximates the dynamics of SGD with high accuracy, in particular in large dimension. In our notation, hSGD for empirical risk minimization is given by

$$dX_t = -\gamma \nabla f(X_t) dt + \gamma \sqrt{\frac{2}{n^2 B} L(X_t) \nabla^2 L(X_t)} dW_t, \quad (\text{hSGD})$$

²Full derivation given in Supplement A.1.

where $(W_t)_{t \geq 0}$ is d -dimensional standard Brownian motion³.

Following Paquette et al. [2022a], the stochastic differential equation (hSGD) can be simplified by using the singular value decomposition of the design matrix A . In detail, let $A = P\Sigma Q^T$ be the singular value decomposition of A , where Q is d -by- d and satisfies $Q^T Q = I$, P is n -by- d and satisfies $P^T P = I$ and

$$\Sigma = \text{diag}\{\lambda_j\}, \quad \lambda_1 \geq \lambda_2 \geq \dots \geq \lambda_d \geq 0.$$

At this point we impose the following mild assumption:

Assumption 2.1. All Eigenvalues of A are strictly positive and b is not in the column space of A .

It is easily verified that under Assumption 2.1 $x^* = (A^T A)^{-1} A^T b$ is the global minimum of the unregularized loss function L . We set

$$\begin{aligned} \alpha &= (\alpha_i)_{i=1}^d = \left[\left(1 - \frac{1}{n} \right) \Sigma^T \Sigma - \delta I_d \right] Q^T x^* \\ \beta &= b^T (P P^T - I) b > 0 \\ Y_t &= (Y_t^i)_{i=1}^d = Q^T X_t - Q^T x^* \end{aligned}$$

where the strict positivity of β follows from Assumption 2.1, and obtain the system of SDEs

$$\begin{aligned} dY_t^i &= -\gamma \left[\left(\frac{\lambda_i^2}{n} + \delta \right) Y_t^i - \alpha_i \right] dt \\ &\quad + \gamma \lambda_i \sqrt{\frac{1}{Bn^2} \left[\sum_{j=1}^d (\lambda_j Y_t^j)^2 + \beta \right]} dB_t^i \end{aligned} \quad (3)$$

for the ‘centered principal components’ (Y_t^1, \dots, Y_t^d) of (hSGD), on which our analysis will be based. Note that the processes Y_t^i are only coupled through the summation term in their diffusion coefficients.

2.4 Heavy-Tailed Distributions

We start by collecting some definitions related to heavy-tailed distributions and their tail-index (cf. Resnick [2007]).

Definition 2.2. A distribution function $F(z)$ is said to be *heavy-tailed* (at the right end) if and only if

$$\limsup_{t \rightarrow \infty} \frac{1 - F(x)}{e^{-sz}} = \infty, \quad \text{for all } s > 0.$$

A real-valued random variable is said to be heavy-tailed if its distribution function is heavy-tailed.

Definition 2.3. An \mathbb{R}^d -valued random vector X is heavy-tailed if $u^T X$ is heavy-tailed for some vector $u \in \mathbb{S}^{d-1} := \{u \in \mathbb{R}^d : \|u\| = 1\}$.

³We remark that Paquette et al. [2022a] assume a batch size of $B = 1$; the derivation of Mori et al. [2022], however, does not restrict B .

Definition 2.4. The *tail-index* of an \mathbb{R}^d -valued random vector X is defined as

$$\eta := \sup\{p \geq 0 : \mathbb{E}[|X|^p] < \infty\} \in [0, \infty]$$

In particular, a finite tail-index $\eta < \infty$ implies heavy-tailedness of X , and lower values of η signify increased heaviness of tails and more extremal behavior. A tail-index of $\eta < 2$, for example, implies infinite variance and $\eta < 1$ implies non-existence of even the mean of X . Examples of heavy-tailed distributions are the lognormal distribution, the t -distribution, the Pareto (power-law) distribution, and α -stable distributions.

Finally, we introduce a definition related to the asymptotic behavior of stochastic processes.

Definition 2.5. Let $X = (X_t)_{t \geq 0}$ be a stochastic process. The *asymptotic tail-index* of X is defined as

$$\eta := \sup\{p \geq 0 : \limsup_{t \rightarrow \infty} \mathbb{E}[|X_t|^p] < \infty\}. \quad (4)$$

2.5 Pearson Diffusions

We perform a convenient rescaling of (3) by setting, for $i \in \{1, \dots, d\}$,

$$\begin{aligned} Z_t^i &= \frac{\lambda_i}{\sqrt{\beta}} Y_t^i, \quad \theta_i = \gamma \left(\frac{\lambda_i^2}{n} + \delta \right) > 0, \\ \mu_i &= \frac{n \lambda_i \alpha_i}{\sqrt{\beta} (\lambda_i^2 + n \delta)}, \quad a_i = \frac{\gamma \lambda_i^4}{2nB (\lambda_i^2 + n \delta)}, \end{aligned} \quad (5)$$

which recasts the system (3) to

$$dZ_t^i = -\theta_i (Z_t^i - \mu_i) dt + \sqrt{2\theta_i a_i (|Z_t^i|^2 + 1)} dB_t^i. \quad (6)$$

These SDEs now have a clear structural resemblance to the system of independent one-dimensional SDEs

$$d\hat{Z}_t^i = -\theta_i (\hat{Z}_t^i - \mu_i) dt + \sqrt{2\theta_i a_i ((\hat{Z}_t^i)^2 + 1)} dB_t^i, \quad (7)$$

with the only difference given by the coupling of (6) through the $|Z_t^i|^2$ -term in the diffusion coefficient. The components of (7) are independent *Pearson diffusions*. Pearson diffusions are a flexible class of SDEs with a unified theory for statistical inference and with stationary distributions known as Pearson distributions (cf. Forman and Sørensen [2008]). The stationary distribution of \hat{Z}_t^i described by (7) is called Pearson’s type IV distribution (or skew t -distribution) and has the un-normalized density

$$\begin{aligned} p_i(u) &\propto \left[1 + \left(\frac{u}{\sqrt{\nu_i}} + \mu_i \right)^2 \right]^{-\frac{\nu_i+1}{2}} \\ &\quad \exp \left\{ \mu_i (\nu_i - 1) \arctan \left(\frac{u}{\sqrt{\nu_i}} + \mu_i \right) \right\} \end{aligned} \quad (8)$$

with $\nu_i = a_i^{-1} + 1$. If $\mu_i = 0$, Pearson’s type IV distribution will be a scaled t -distribution. Figure 1 (g) demonstrates

the change in the complementary cumulative distribution functions of the t -distribution as ν_i increases. It is easily seen that the Pearson type IV distribution is heavy-tailed with tail-index given by ν_i , thus providing a first connection between the SDE-approach and the emergence of heavy-tails. We also emphasize the contrast to Gurbuzbalaban et al. [2021], where the different class of α -stable distributions is used to describe the asymptotic behavior of SGD iterates.

3 Theoretical results

3.1 Comparison to Pearson Diffusion

Theorem 3.1. *For $i = 1, \dots, d$, let $(Z_t^i)_{t \geq 0}$ be the components of the rescaled (hSGD) from (6) and $(\hat{Z}_t^i)_{t \geq 0}$ be the independent Pearson diffusion from (7). Then for any $t \geq 0$ and convex function $g : \mathbb{R} \rightarrow \mathbb{R}$ it holds that*

$$\mathbb{E}[g(Z_t^i)] \geq \mathbb{E}[g(\hat{Z}_t^i)]. \quad (9)$$

In particular this implies the ordering of p -moments

$$\mathbb{E}[|Z_t^i|^p] \geq \mathbb{E}[|\hat{Z}_t^i|^p] \quad (10)$$

for all $p \geq 1$.

The ordering of Z_t^i and \hat{Z}_t^i given by (9) is also known as *convex stochastic order*; see Shaked and Shanthikumar [2007]. Note that finiteness of the expectations does not need to be assumed, i.e., the inequalities also hold if one of the expectations takes the value $+\infty$. Comparison results in stochastic order for SDEs have been shown for example in Bergenthum and Rüschemdorf [2007]. However, since none of the results can be applied directly in our setting, we will give a self-contained proof.

Comparison results for SDEs generally require two conditions (cf. Bergenthum and Rüschemdorf [2007]): An ordering between the drift- and diffusion-coefficients of the two SDEs, and the ‘propagation-of-order’-property for one of the processes. In our case, the SDEs (6) and (7) can be represented – component by component – in the form

$$\begin{aligned} dZ_t^i &= b_i(Z_t)dt + \sigma_i(Z_t)dB_t^i, \\ d\hat{Z}_t^i &= b_i(\hat{Z}_t)dt + \hat{\sigma}_i(\hat{Z}_t)dB_t^i, \end{aligned}$$

where

$$\begin{aligned} b_i(z) &= -\theta_i(z_i - \mu_i), \\ \sigma_i^2(z) &= 2\theta_i a_i(|z|^2 + 1) \quad \text{and} \quad \hat{\sigma}_i^2(z_i) = 2\theta_i a_i(z_i^2 + 1). \end{aligned}$$

While the drift coefficients are identical, the diffusion coefficients satisfy the inequality $\sigma_i(z) \geq \hat{\sigma}_i(z)$ for all $z \in \mathbb{R}^d$ and $i = 1, \dots, d$. Also note that all coefficients are Lipschitz continuous and of bounded growth, such that the standard

assumptions for uniqueness and existence of strong SDE solutions are satisfied. Moreover, the SDEs for \hat{Z}_t^i are decoupled and each is a Markov diffusion with generator given by

$$\hat{\mathcal{L}}_i = b_i(x)\partial_x + \frac{\sigma_i(x)^2}{2}\partial_{xx},$$

where x denotes the scalar state variable of \hat{Z}^i . Let $C_P^l(\mathbb{R})$ denote the subspace of C^l -functions for which all derivatives up to order l have polynomial growth. Suppose that $g \in C_P^l(\mathbb{R})$. From Theorem 4.8.6 in Kloeden and Platen [1999] the backward functional

$$\mathcal{G}_i(t, x) = \mathbb{E}[g(\hat{Z}_T^i) | \hat{Z}_t^i = x], \quad t \in [0, T],$$

satisfies the backward Kolmogorov equation

$$\begin{aligned} \partial_t \mathcal{G}_i(t, x) + \hat{\mathcal{L}}_i \mathcal{G}_i(t, x) &= 0 \quad t < T, \\ \mathcal{G}_i(T, x) &= g(x). \end{aligned} \quad (11)$$

with $\partial_t \mathcal{G}_i$ continuous and $\mathcal{G}_i(t, \cdot) \in C_P^l(\mathbb{R})$ for each $t \in [0, T]$. The following Lemma on the *propagation-of-order* property of \hat{Z} can be shown by Euler-Maruyama approximation; see Supplement A.2 for the complete proof.

Lemma 3.2. *If $g \in C_P^l(\mathbb{R})$ is convex, so is $\mathcal{G}_i(t, \cdot)$ for all $t \in [0, T]$ and $i = 1, \dots, d$.*

Finally, we need a technical result that shows that each process $\mathcal{G}_i(z, \hat{Z}_t^i)_{t \in [0, T]}$ is of ‘class (D)’ a proof is given in the Supplement A.2.⁴

Lemma 3.3. *For each $i = 1, \dots, d$, the process $\mathcal{G}_i(t, Z_t^i)_{t \in [0, T]}$ is of class (D).*

We are now prepared to give the proof of our first main result.

Proof of Theorem 3.1. Let g be a convex function and assume for now that $g \in C_P^2(\mathbb{R})$. Define the local martingale

$$L_t = \int_0^t \partial_x \mathcal{G}_i(s, Z_s^i) \sigma_i(Z_s) dB_s^i$$

Using Itô’s formula in the first step and (11) in the second step, we have

$$\begin{aligned} &\mathcal{G}_i(t, Z_t^i) - \mathcal{G}_i(0, Z_0^i) \\ &= \int_0^t \partial_t \mathcal{G}_i(s, Z_s^i) ds + \\ &\quad \int_0^t \left(b_i(Z_t^i) \partial_x + \frac{\sigma_i^2(Z_t)}{2} \partial_{xx} \right) \mathcal{G}_i(s, Z_s^i) ds + L_t \\ &= - \int_0^t \hat{\mathcal{L}}_i \mathcal{G}_i(s, Z_s) ds + \\ &\quad \int_0^t \left(b_i(Z_t^i) \partial_x + \frac{\sigma_i^2(Z_t)}{2} \partial_{xx} \right) \mathcal{G}_i(s, Z_s^i) ds + L_t \\ &= \frac{1}{2} \int_0^t [\sigma_i^2(Z_s) - \hat{\sigma}_i^2(Z_s^i)] \partial_{xx} \mathcal{G}_i(s, Z_s^i) ds + L_t. \end{aligned} \quad (12)$$

⁴A stochastic process $(X_t)_{t \in I}$ is of class (D), if the set $\{X_\tau : \tau \text{ is } I\text{-valued stopping time}\}$ is uniformly integrable (cf. Definition 4.8 in Karatzas and Shreve [2012]).

By $\mathcal{G}_i(t, \cdot) \in C_P^2(\mathbb{R})$ and Lemma 3.2 we obtain $\partial_{xx}\mathcal{G}_i(s, \cdot) \geq 0$ for all $i \in \{1, \dots, d\}$. Thus, due to the ordering of σ_i^2 and $\hat{\sigma}_i^2$, the first term in the right hand side of (12) is nonnegative. Since L is a continuous local martingale with zero initial data, it follows that $\mathcal{G}_i(t, Z_t) - \mathcal{G}_i(0, Z_0)$ is a local submartingale.

Let τ_n be a localizing sequence for $\mathcal{G}_i(t, Z_t)$. For all $t \in [0, T]$, we have

$$\mathcal{G}_i(t \wedge \tau_n, Z_{t \wedge \tau_n}) - \mathcal{G}_i(0, Z_0) \xrightarrow[n \rightarrow \infty]{a.s.} \mathcal{G}_i(t, Z_t) - \mathcal{G}_i(0, Z_0). \quad (13)$$

Since $\mathcal{G}_i(t, Z_t)$ is a process of class (D) or locally L^p -bounded, $p > 1$, it follows that $\mathcal{G}_i(t \wedge \tau_n, Z_{t \wedge \tau_n}) - \mathcal{G}_i(0, Z_0)$ is uniformly integrable. Combining almost-sure convergence with the uniformly integrable property, it implies that the convergence (13) also takes place in L^1 , and therefore, $\mathcal{G}_i(t, Z_t) - \mathcal{G}_i(0, Z_0)$ is a submartingale. By taking expectations on both sides of (12) and using the fact that $Z_0 = \hat{Z}_0$, we obtain the comparison result

$$\mathbb{E}g(Z_T^i) = \mathbb{E}\mathcal{G}_i(T, Z_T^i) \geq \mathcal{G}(0, Z_0^i) = \mathbb{E}[g(\hat{Z}_T^i)] \quad (14)$$

for all convex $g \in C_P^2(\mathbb{R})$.

Now let g be arbitrary convex function on \mathbb{R} . From Theorem 3.1.4 in Hiriart-Urruty and Lemaréchal [1996] we can find, for each $n \in \mathbb{N}$ a convex Lipschitz function \tilde{g}_n such that $\tilde{g}_n \leq g$ in $[-n, n]$ and $\tilde{g}_n \leq g$ in $\mathbb{R} \setminus [-n, n]$. By Azagra [2013] we can find further smooth convex functions $g_n \in C_{\text{Lip}}^\infty(\mathbb{R})$ such that $\tilde{g}_n - \frac{1}{n} \leq g_n \leq \tilde{g}_n$ on all of \mathbb{R} . It follows that the sequence g_n converges pointwise to g from below. We observe that $C_{\text{Lip}}^\infty(\mathbb{R}) \subset C_P^2(\mathbb{R})$ and equation (9) now follows from (14) by monotone convergence. Finally, equation (10) follows by choosing the convex function $g(z_i) = |z_i|^p$. \square

3.2 Upper bound for the asymptotic tail-index

From $X_t = QY_t + x_*$, the triangle inequality and the unitary invariance of the Euclidean norm, it follows that $|Y_t| \leq |X_t| + |x_*|$. Thus, we have

$$\begin{aligned} \frac{\beta^{p/2}}{\lambda_1^p} \mathbb{E}[|Z_t^1|^p] &= \mathbb{E}[|Y_t^1|^p] \leq \mathbb{E}[|Y_t|^p] \\ &\leq 2^p (\mathbb{E}[|X_t|^p] + |x_*|^p). \end{aligned} \quad (15)$$

Now, let $p > \nu_1$. By Theorem 3.1, Fatou's Lemma, and the properties of the skew t -distribution (8)

$$\begin{aligned} \limsup_{t \rightarrow \infty} \mathbb{E}[|Z_t^1|^p] &\geq \liminf_{t \rightarrow \infty} \mathbb{E}[|Z_t^1|^p] \\ &\geq \liminf_{t \rightarrow \infty} \mathbb{E}[|\hat{Z}_t^1|^p] \geq [|\hat{Z}_\infty^1|^p] = \infty. \end{aligned} \quad (16)$$

Together with (15) this implies that also

$$\limsup_{t \rightarrow \infty} \mathbb{E}[|X_t|^p] = \infty,$$

and it follows from (4) that the asymptotic tail-index satisfies $\eta \leq p$ for all $p > \nu_1$. Finally, the parameter ν_1 in the limit distribution of \hat{Z}^1 is given by $\nu_1 = 1 + a_1^{-1}$, where a_1 can be found in (5). Thus, we immediately obtain the following result.

Theorem 3.4. *The asymptotic tail-index η of (hSGD) has the upper bound*

$$\eta \leq \eta^* := 1 + \frac{2nB(\lambda_1^2 + n\delta)}{\gamma\lambda_1^4}. \quad (17)$$

3.3 Lower bound for the asymptotic tail-index

For better readability, we rewrite (hSGD) as the following form

$$dX_t = F(X_t)dt + G(X_t)dB_t \quad (18)$$

with

$$\begin{aligned} F(X_t) &= -\gamma \left[\frac{1}{n} A^\top (AX_t - b) + \delta X_t \right], \\ G(X_t) &= \gamma \sqrt{\frac{1}{n^2 B} \|AX_t - b\|^2 A^\top A}. \end{aligned}$$

Under a certain assumption on the learning rate, we can prove (see Supplement A.3 for details) that for all $\rho \in (0, \eta_*)$

$$\begin{aligned} \limsup_{|x| \rightarrow \infty} \frac{(1 + |x|^2) [2x^\top F(x) + |G(x)|^2] - (2 - \rho)|x^\top G(x)|^2}{|x|^4} \\ < -C_1, \end{aligned} \quad (19)$$

where C_1 is a positive constant and

$$\eta_* := 1 + \frac{2n(\lambda_1^2 + n\delta)}{\gamma\lambda_1^4} - \frac{\sum_{i=2}^d \lambda_i^2}{\lambda_1^2} > 0.$$

By Theorem 5.2 in Li et al. [2019], the solution X_t of the SDE (18) satisfies

$$\sup_{0 \leq t < \infty} \mathbb{E}|X_t|^\rho \leq C_2$$

with C_2 a positive constant. Then we have the following theorem.

Theorem 3.5. *Suppose that the learning rate γ satisfies*

$$\gamma < \bar{\gamma} := \frac{2nB(\lambda_1^2 + n\delta)}{\lambda_1^2 \sum_{i=1}^d \lambda_i^2},$$

then the asymptotic tail-index η of (hSGD) has the lower bound

$$1 + \frac{2nB(\lambda_1^2 + n\delta)}{\gamma\lambda_1^4} - \frac{\sum_{i=2}^d \lambda_i^2}{\lambda_1^2} = \eta_* \leq \eta. \quad (20)$$

3.4 Discussion of theoretical results

In comparison to Gurbuzbalaban et al. [2021], we note the following differences and similarities. In our setting, the data distribution is completely arbitrary, since all results are given conditional on the data matrix A . In Gurbuzbalaban et al. [2021] on the other hand, the more restrictive assumption of an isotropic Gaussian data distribution is made. Moreover, our tail-index bounds (17) and (20) are quantitative and explicit, whereas Gurbuzbalaban et al. [2021] describe when a phase transition of the asymptotic tail-index η from $\eta < 2$ to $\eta > 2$ occurs, but do not give further quantitative estimates of η .

Some further interesting observations can be made when we consider the dependency of η on the meta-parameters of the stochastic gradient descent procedure:

Corollary 3.6. *The upper and lower bounds of the tail-index are increasing in the regularization parameter δ and batch size B , and are decreasing in the learning rate γ and the first singular value λ_1 of the data matrix A .*

This result agrees with Theorem 4 in Gurbuzbalaban et al. [2021], obtained under the assumption of an isotropic data distribution $a_i \sim N(0, \sigma^2 I_d)$, in all aspects, except the dependency on dimension d .⁵ While Gurbuzbalaban et al. [2021] report decreasing dependency on d , our tail-index bounds do not explicitly depend on dimension d . Nevertheless, the two results can be reconciled as follows: Under the assumptions in Gurbuzbalaban et al. [2021], the data matrix $A = (a_i)$ is random with $\mathbb{E}(A^T A) = \sigma^2 I_d$, and the product matrix $W := A^T A$ follows the so-called Wishart ensemble (cf. Wishart [1928]). Moreover, from Theorem 1.1 in Johnstone [2001] it follows that for large d the maximum eigenvalue of W is

$$\lambda_1^2 = \sigma^2 \left[\left(\frac{1}{\sqrt{r}} + 1 \right)^2 d + r^{\frac{1}{6}} \left(\frac{1}{\sqrt{r}} + 1 \right)^{\frac{4}{3}} d^{\frac{1}{3}} \chi \right], \quad (21)$$

where the ratio $r = \frac{d}{n-1} < 1$ and the distribution function of the random variable χ is the well-known Tracy-Widom distribution of order 1 (cf. Tracy and Widom [1996]). From (21), we can calculate the average of λ_1^2 as

$$\mathbb{E}[\lambda_1^2] = \sigma^2 \left(\frac{1}{\sqrt{r}} + 1 \right)^2 d = \sigma^2 (\sqrt{n-1} + \sqrt{d})^2$$

and λ_1^2 fluctuates around this expectation over a narrow region of width $O(d^{\frac{1}{3}})$. Substituting λ_1^2 by its expectation in (17) and (20) we can now see that η_* and η^* decrease in both variance σ^2 and d , consistent with Gurbuzbalaban et al. [2021].

⁵With the key difference that (17) and (20) give a *quantitative* description of all dependencies, while Gurbuzbalaban et al. [2021] is only *qualitative* in nature.

4 Experiments

Based on the upper and lower bounds in Theorems 3.4 and 3.5, we present some experiments to illustrate the tail behavior of SGD and the factors influencing the tail-index. The procedure of our experiments contains the following steps.

1. Given [data| b], we transform the data to be on a similar scale by the linear scaling

$$A = \frac{\text{data} - \min\{\text{data}\}}{\max\{\text{data}\} - \min\{\text{data}\}}.$$

2. Let K be the iteration number of SGD. We apply SGD to solve ERM. The final state $x_K \in \mathbb{R}^d$ is a random vector.
3. Repeat the second step 1000 times for different initial points and obtain 1000 different samples of x_K .
4. For further distributional analysis we project x_K via $y = q_1^\top x_K$ on the dominant direction, given by the first right singular vector q_1 of A . Then we utilize the 1000 samples to obtain the empirical complementary cumulative distribution function (ccdf) of y .

4.1 Datasets

Synthetic data. We first validate our results in the same synthetic setup used in Gurbuzbalaban et al. [2021]. All data points are drawn from isotropic Gaussian distributions, precisely, the i -th row of $\mathcal{X} \in \mathbb{R}^{n \times d}$ contains $\chi_i \in \mathbb{R}^d \sim \mathcal{N}(0, I_d)$. Then given $x \in \mathbb{R}^d \sim \mathcal{N}(0, 3I_d)$ we draw the response vector $b \in \mathbb{R}^n$ with components $b_i \sim \mathcal{N}(\chi_i x, 3)$. We set the number n of the synthetic data to be 2000 through our experiments.

Real data. In our second setup we conduct our experiments on the handwritten digits dataset from the Scikit-learn python package (cf. Pedregosa et al. [2011]) and a random feature model proposed in Rahimi and Recht [2007]. The digits dataset contains $n = 1797$ images of handwritten digits in a 8×8 pixel format. The pixels are stacked into vectors of length $n_0 = 8^2 = 64$ resulting in a raw data matrix $\mathcal{Y} \in \mathbb{R}^{n \times n_0}$ and the class label $b_i = \{0, 1, \dots, 9\}$ is used as response vector. For the random feature model, we choose a dimension d and draw a random weight matrix $W \in \mathbb{R}^{n_0 \times d}$ having standard Gaussian entries. The feature matrix $W \in \mathbb{R}^{n \times d}$ is given by

$$\mathcal{Z} = \sigma \left(\frac{\mathcal{Y}W}{\sqrt{n_0}} \right) \in \mathbb{R}^{n \times d},$$

where $\sigma(\cdot)$ is a rescaled ReLU activation function.

Parameters. Tables 1 and 2 contain all parameter values used for the figures.

Table 1: Parameters used for Figure 1

Figure 1	data	d	K	γ	$\overline{\gamma}$	δ	B	λ_1	η_*	η^*
(a), (d), (h)	\mathcal{X}	200	1000	0.015	0.037	0	1	319.83	3.56	3.61
(b), (e), (i)	\mathcal{Y}	64	10000	0.100	0.133	0	1	137.07	2.48	2.91
(c), (f), (j)	\mathcal{Z}	200	10000	0.200	0.304	0	1	93.49	2.70	3.06

Table 2: Parameters used for Figure 2

Figure 2	data	d	K	γ	δ	B	λ_1
(a)	\mathcal{X}	200	1000	0.010 to 0.025	0	1	353.10
(b)	\mathcal{X}	200	1000	0.10	0	1 to 4	319.83
(c)	\mathcal{X}	100 to 260	1000	0.02	0	1	223.05 to 360.08
(d)	\mathcal{Z}	200	10000	0.10 to 0.25	0	1	93.49
(e)	\mathcal{Z}	200	10000	0.10	0	1 to 4	93.49
(f)	\mathcal{Z}	80 to 360	10000	0.20	0	1	58.25 to 106.61

4.2 Empirical results

Heavy tailed behavior. To verify the heavy-tailed behavior of y as well as our tail-index bounds from Theorems 3.4 and 3.5 and the distributional approximation suggested by (8), we use MLE-estimation to fit our centered data as

$$z := y - \text{mean}\{y\} \sim \kappa t(\nu).$$

where $t(\nu)$ denotes a t-distribution with parameter ν and κ is a scaling factor.⁶ The QQ-plots in Figure 1(a), (b) and (c) show that the t-distribution provides an excellent fit to the empirical data, validating our use of Pearson diffusions to approximate SGD. For comparison, we also fit (using MLE-estimation) an α -stable distribution, as suggested in Gurbuzbalaban et al. [2021], to the same data and show the resulting QQ-plots in Figure 1(e), (f) and (g). It can be seen that the fitted α -stable distribution massively overestimates the heaviness of tails, in particular for the random feature model on real data. We complement these figures by a Kolmogorov-Smirnov test (cf. Chapter 4.4 in Corder and Foreman [2014]) testing for the goodness-of-fit of the t-distribution and the α -stable distribution respectively; see Table 3 for results.

Moreover, in Figure 1(h), (i) and (j) we plot (in doubly logarithmic coordinates) the empirical cdf of the SGD iterates z , together with the cdf of the t-distribution parametrized by our lower and upper bound η_* and η^* . It can be seen that the empirical cdf, including its tail, is nicely sandwiched between upper and lower bound, validating Theorems 3.4 and 3.5. Additionally, we once more confirm the heavy-tailed behavior of SGD iterates as already observed in Simsekli et al. [2019], Hodgkinson and Mahoney [2021], Gurbuzbalaban et al. [2021].

Increasing learning rate / Decreasing batch size. To illustrate the effect of the learning rate γ , we perform a set of experiments with constant batch size $B = 1$, varying only the learning rate γ . Meanwhile, by fixing γ , we conduct a series of experiments with varying B . In Figure 2 (a),(b),

⁶Eq. (8) actually implies a skew t-distribution, but we use a symmetric one to avoid the estimation of an additional parameter μ .

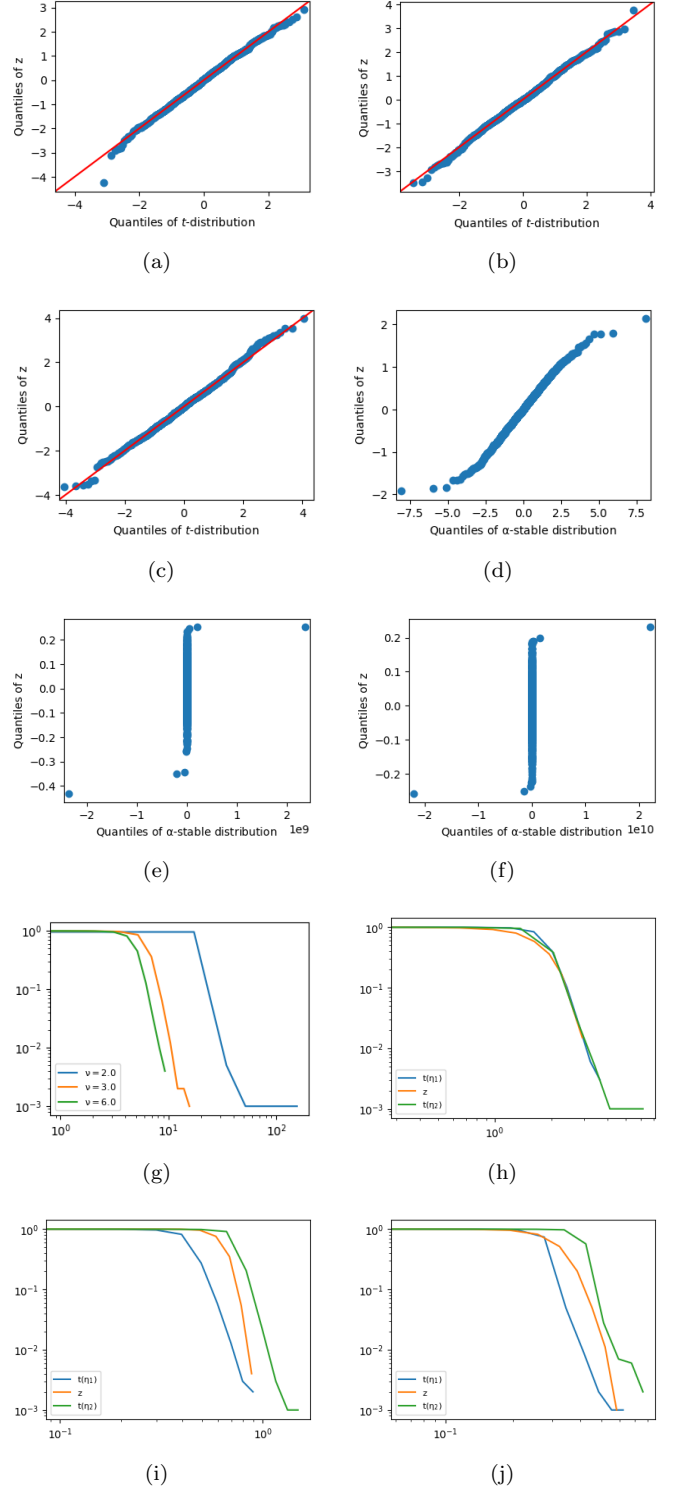


Figure 1: (a)-(c) Quantile-Quantile plots of fitted t-distribution against empirical SGD iterates; (d)-(f) Quantile-Quantile plots of fitted α -stable distribution against empirical SGD iterates. (g) Complementary cumulative distribution function (ccdf) of t-distribution with different tail indices; (h)-(j) Comparison between ccdf of empirical data and t-distribution parameterized by upper tail-index bound η^* and lower bound η_* .

Table 3: Kolmogorov-Smirnov test. The null hypothesis H_0 is that two distributions are identical, the alternative H_1 is that they are not identical. For the t-distribution we use one-sided null hypothesis $\overline{H}_0: F_z(x) \geq F_{\kappa t(\eta^*)}(x)$ for x , the alternative $\overline{H}_1: F_z(x) < F_{\kappa t(\eta^*)}(x)$ for at least one x ; The one-sided null hypothesis $\underline{H}_0: F_z(x) \leq F_{\kappa t(\eta_*)}(x)$ for all x , the alternative $\underline{H}_1: F_z(x) > F_{\kappa t(\eta_*)}(x)$ for at least one x .

Figure 1	κ	hypothesis	K-S statistic	p-value	decision
(d)	1.0	H_0, H_1	0.6	0.052 > 0.05	not reject H_0
(e)	1.0	H_0, H_1	0.8	0.002 < 0.05	reject H_0
(f)	1.0	H_0, H_1	0.9	0.0002 > 0.05	reject H_0
(h)	0.320	$\overline{H}_0, \overline{H}_1$ $\underline{H}_0, \underline{H}_1$	0.2 0.0	0.68 > 0.05 1.00 > 0.05	not reject \overline{H}_0 not reject \underline{H}_0
(i)	0.045	$\overline{H}_0, \overline{H}_1$ $\underline{H}_0, \underline{H}_1$	0.1 0.1	0.91 > 0.05 0.91 > 0.05	not reject \overline{H}_0 not reject \underline{H}_0
(j)	0.050	$\overline{H}_0, \overline{H}_1$ $\underline{H}_0, \underline{H}_1$	0.0 0.3	1.00 > 0.05 0.42 > 0.05	not reject \overline{H}_0 not reject \underline{H}_0

(d) and (e) we can see that increasing γ and decreasing B leads to decreasing tail-index η .

Increasing dimension. The dimension d affects the upper and lower bounds via the leading singular value λ_1 of data matrix A constructed by \mathcal{X} (see the discussion in Section 3.4), although it does not appear explicitly in η^* and η_* . In Figure 2 (c) and (f), we explore the effect of varying d and observe that increasing d gives increasing λ_1 which results in decreasing tail-index η .

5 Conclusion

We have introduced a new method, namely a comparison result in convex stochastic order for homogenized stochastic gradient descent, to obtain explicit upper bounds for the tail-index of stochastic gradient descent. These upper bounds are complemented by lower bounds obtained from results on moment stability of stochastic differential equations. Together, these bounds confirm the heavy-tailed nature of neural network parameters under optimization by SGD and provide insights into the dependency between their tail-index and optimization meta-parameters. One limitation of the method is that we have derived it only for plain SGD with constant learning rate. In future research, the method could be adapted to more advanced optimization methods involving momentum and adaptive choice of learning rate.

References

- D. Azagra. Global and fine approximation of convex functions. *Proceedings of the London Mathematical Society*, 107(4): 799–824, 2013.
- J. Bergenthum and L. Rüschemdorf. Comparison of semi-martingales and Lévy processes. *The Annals of Probability*, 35(1):228–254, 2007.

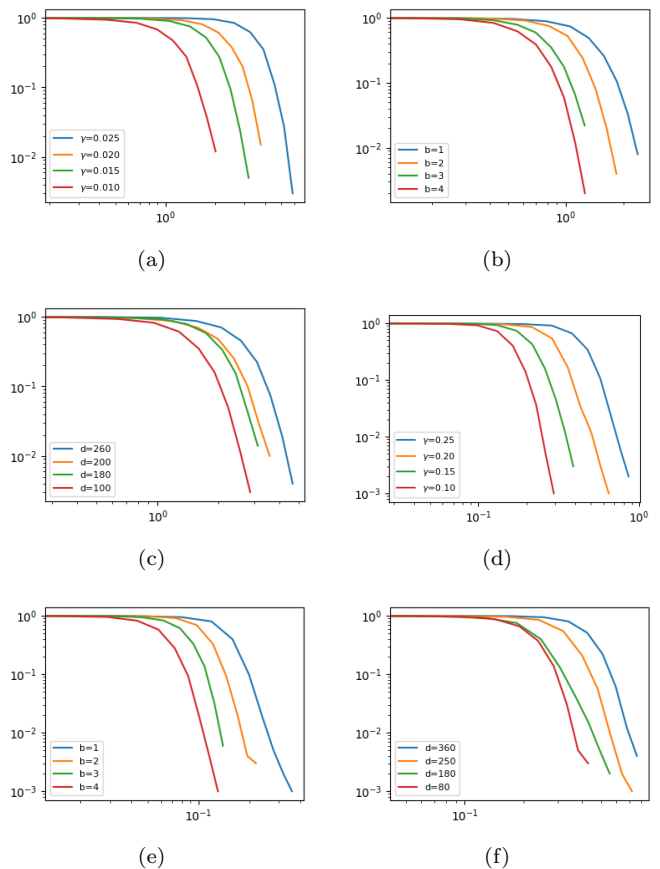


Figure 2: Empirical complementary cumulative distribution functions on log-log scale for the effect of varying parameters.

- L. Bottou, E. F. Curtis, and J. Nocedal. Optimization methods for large-scale machine learning. *SIAM Review*, 60(2):223–311, 2018.
- G.W. Corder and D.I. Foreman. *Nonparametric Statistics: A Step-by-Step Approach*. Wiley, 2014.
- Christa Cuchiero, Martin Keller-Ressel, and Josef Teichmann. Polynomial processes and their applications to mathematical finance. *Finance and Stochastics*, 16:711–740, 2012.
- Damir Filipović and Martin Larsson. Polynomial diffusions and applications in finance. *Finance and Stochastics*, 20: 931–972, 2016.
- Julie Forman and Michael Sørensen. The Pearson diffusions: a class of statistically tractable diffusion processes. *Scandinavian Journal of Statistics*, 35:438–465, 2008.
- I. Goodfellow, Y. Bengio, and A. Courville. *Deep learning*. MIT Press, 2016.
- Mert Gurbuzbalaban, Umut Simsekli, and Lingjiong Zhu. The heavy-tail phenomenon in SGD. In *International Conference on Machine Learning*, pages 3964–3975, 2021.
- Trevor Hastie, Robert Tibshirani, and Jerome Friedman. *The Elements of Statistical Learning*. Springer, 2009.
- J.-B. Hiriart-Urruty and C. Lemaréchal. *Convex analysis and minimization algorithms I: Fundamentals*. Springer, 1996.
- L. Hodgkinson and M. Mahoney. Multiplicative noise and heavy tails in stochastic optimization. In *International Conference on Machine Learning*, pages 4262–4274, 2021.
- Roger A Horn and Charles R Johnson. *Matrix analysis*. Cambridge university press, 2012.
- S. Jastrzebski, Z. Kenton, D. Arpit, N. Ballas, A. Fischer, Y. Bengio, and A. Storkey. Three factors influencing minima in SGD. *arXiv:1711.04623*, 2017.
- Iain M. Johnstone. On the distribution of the largest eigenvalue in principal components analysis. *The Annals of Statistics*, 29(2):295–327, 2001.
- I. Karatzas and S. Shreve. *Brownian motion and stochastic calculus*. Springer, 2012.
- Peter E. Kloeden and Eckhard Platen. *Numerical Solution of Stochastic Differential Equations*. Springer, 1999.
- Xiaoyue Li, Xuerong Mao, and George Yin. Explicit numerical approximations for stochastic differential equations in finite and infinite horizons: truncation methods, convergence in p -th moment and stability. *IMA journal of Numerical Analysis*, 39:847–892, 2019.
- S. Mandt, M. Hoffman, and D. A. Blei. A variational analysis of stochastic gradient algorithms. In *International Conference on Learning Representations*, 2016.
- C. Martin and M. Mahoney. Traditional and heavy tailed self regularization in neural network models. In *International Conference on Machine Learning*, pages 4284–4293, 2019.
- T. Mori, Ziyin Li, K. Liu, and M. Ueda. Power-law escape rate of SGD. In *International Conference on Machine Learning*, pages 15959–15975, 2022.
- Alfred Müller and Dietrich Stoyan. *Comparison Methods for Stochastic Models and Risks*. Wiley, 2002.
- Courtney Paquette, Elliot Paquette, Ben Adlam, and Jeffrey Pennington. Homogenization of SGD in high-dimensions: Exact dynamics and generalization properties. *Advances in Neural Information Processing Systems*, 35:35984–35999, 2022a.
- Courtney Paquette, Elliot Paquette, Ben Adlam, and Jeffrey Pennington. Implicit regularization or implicit conditioning? exact risk trajectories of sgd in high dimensions. *Advances in Neural Information Processing Systems*, 35: 35984–35999, 2022b.
- Fabian Pedregosa, Gaël Varoquaux, Alexandre Gramfort, Vincent Michel, Bertrand Thirion, Olivier Grisel, Mathieu Blondel, Peter Prettenhofer, Ron Weiss, Vincent Dubourg, Jake Vanderplas, Alexandre Passos, David Cournapeau, Matthieu Brucher, Matthieu Perrot, and Édouard Duchesnay. Scikit-learn: Machine learning in python. *Journal of Machine Learning Research*, 12(85):2825–2830, 2011.
- A. Rahimi and B. Recht. Random features for large-scale kernel machines. In *Advances in Neural Information Processing Systems*, 2007.
- S. I. Resnick. *Heavy-tail phenomena: probabilistic and statistical modeling*. Springer, 2007.
- M. Shaked and J. G. Shanthikumar. *Stochastic orders*. Springer, 2007.
- Umut Simsekli, L. Sagun, and Mert Gurbuzbalaban. A tail-index analysis of stochastic gradient noise in deep neural networks. In *International Conference on Machine Learning*, pages 5287–5837, 2019.
- Umut Simsekli, O. Sener, G. Deligiannidis, and M. A. Erdogdu. Hausdorff dimension, heavy tails, and generalization in neural networks. In *Advances in Neural Information Processing Systems*, pages 5138–5151, 2020.
- Samuel L Smith and Quoc V Le. A Bayesian perspective on generalization and stochastic gradient descent. In *International Conference on Learning Representations*, 2018.

Volker Strassen. The existence of probability measures with given marginals. *The Annals of Mathematical Statistics*, 36:432–439, 1965.

Craig A. Tracy and Harold Widom. On orthogonal and symplectic matrix ensembles. *Communications in Mathematical Physics*, 177:727–754, 1996.

John Wishart. The generalized product moment distribution in samples from a normal multivariate population. *Biometrika*, 20A(1/2):32–52, 1928.

A Supplementary material

A.1 Covariance matrix

Consider the minibatch stochastic gradient

$$\nabla \tilde{f}_k(x) = \frac{1}{B} \sum_{i \in \Omega_k} \nabla f_i(x) = \frac{1}{B} \sum_{i \in \Omega_k} \nabla L_i(x) + \delta x.$$

where B is the batchsize and the random set $\Omega_k = \{i_1, \dots, i_B\}$ consists of B independently identically distributed random integers sampled uniformly from $\{1, 2, \dots, n\}$.

Let $\nabla \tilde{L}_k(x) = \frac{1}{B} \sum_{i \in \Omega_k} \nabla L_i(x)$. It can be rewritten as

$$\nabla \tilde{L}_k(x) = \frac{1}{B} \sum_{i=1}^n \nabla L_i(x) s_i,$$

where the random variable $s_i = l$ if l -multiple i 's are sampled in Ω_k , with $0 \leq l \leq B$. The probability of $s_i = l$ is given by the multinomial distribution $\mathbb{P}(s_i = l) = C_B^l \left(\frac{1}{n}\right)^l \left(1 - \frac{1}{n}\right)^{B-l}$. Moreover, we have

$$\mathbb{E}[s_i] = \frac{B}{n}, \quad \mathbb{E}[s_i s_j] = \frac{B(B-1)}{n^2}, \quad \mathbb{E}[s_i s_i] = \frac{Bn + B(B-1)}{n^2}.$$

We can also compute

$$\mathbb{E}[\nabla \tilde{L}_k(x)] = \frac{1}{B} \sum_{i=1}^n \nabla L_i(x) \mathbb{E}[s_i] = \frac{1}{n} \nabla L(x) \quad (22)$$

and

$$\begin{aligned} & \mathbb{E}[\nabla \tilde{L}_k(x)^T \nabla \tilde{L}_k(x)] \\ &= \frac{1}{B^2} \mathbb{E} \left[\sum_{i=1}^n \sum_{j=1}^n \nabla L_i(x)^T \nabla L_j(x) s_i s_j \right] = \frac{1}{B^2} \sum_{i=1}^n \sum_{j=1}^n [\nabla L_i(x)^T \nabla L_j(x) \mathbb{E}(s_i s_j)] \\ &= \frac{1}{B^2} \sum_{i,j=1}^n \nabla L_i(x)^T \nabla L_j(x) \frac{B(B-1)}{n^2} \\ & \quad + \frac{1}{B^2} \sum_{i=1}^n \nabla L_i(x)^T \nabla L_i(x) \left[\frac{Bn + B(B-1)}{n^2} - \frac{B(B-1)}{n^2} \right] \\ &= \frac{B-1}{B} \frac{1}{n^2} \nabla L(x)^T \nabla L(x) + \frac{1}{nB} \sum_{i=1}^n \nabla L_i(x)^T \nabla L_i(x). \end{aligned} \quad (23)$$

Combining (22) with (23) gives

$$\begin{aligned} C(x) &= \mathbb{E} \left\{ [\nabla \tilde{f}_k(x) - \nabla f(x)]^T [\nabla \tilde{f}_k(x) - \nabla f(x)] \right\} \\ &= \mathbb{E} \left\{ [\nabla \tilde{L}_k(x) - \frac{1}{n} \nabla L(x)]^T [\nabla \tilde{L}_k(x) - \frac{1}{n} \nabla L(x)] \right\} \\ &= \mathbb{E}[\nabla \tilde{L}_k(x)^T \nabla \tilde{L}_k(x)] - \frac{1}{n^2} \nabla L(x)^T \nabla L(x) \\ &= \frac{1}{B} \left[\frac{1}{n} \sum_{i=1}^n \nabla L_i(x)^T \nabla L_i(x) - \frac{1}{n^2} \nabla L(x)^T \nabla L(x) \right]. \end{aligned}$$

A.2 Proofs of some lemmas

Proof of Lemma 3.2. For better readability we suppress the superscript and subscript i in the following SDE

$$d\hat{Z}_t^i = b_i(\hat{Z}_t) dt + \hat{\sigma}_i(\hat{Z}_t) dB_t^i,$$

where $b_i(z) = -\theta_i(z_i - \mu_i)$ and $\hat{\sigma}_i(z_i)^2 = 2\theta_i a_i(z_i^2 + 1)$. We consider its Euler-Maruyama approximation

$$\hat{Z}_{K,t_{j+1}} = \hat{Z}_{K,t_j} + b(\hat{Z}_{K,t_j})\Delta t_j + \hat{\sigma}(\hat{Z}_{K,t_j})(B_{t_{j+1}} - B_{t_j})$$

with $t_j = j\frac{T-t}{K} + t$, $j = \{0, 1, \dots, K\}$ and $\Delta t_j = \frac{T-t}{K} := \Delta$. Using Theorem 9.7.4 in Kloeden and Platen [1999] we have

$$\mathcal{G}_K(t, x) = \mathbb{E}[g(\hat{Z}_{K,T}) | \hat{Z}_{K,t} = x] \rightarrow \mathcal{G}(t, x), \quad t \in [0, T]. \quad (24)$$

Let \mathcal{A} be a transition operator given by

$$\mathcal{A}S = S + \Delta b(S) + \hat{\sigma}(S)W$$

with $W \sim N(0, \Delta)$. We will show that \mathcal{A} satisfies the convex-ordering property

$$\mathbb{E}h(S_1) \leq \mathbb{E}h(S_2) \Rightarrow \mathbb{E}h(\mathcal{A}S_1) \leq \mathbb{E}h(\mathcal{A}S_2) \quad (25)$$

for any convex function $h(\cdot)$. Let S_1, S_2 be random vectors which are independent of W and satisfy $\mathbb{E}h(S_1) \leq \mathbb{E}h(S_2)$. Due to Stassen's theorem in Strassen [1965], we can also assume that $\mathbb{E}(S_2|S_1) = S_1$. It follows from conditional Jensen's inequality that

$$\begin{aligned} \mathbb{E}h(\mathcal{A}S_2) &= \mathbb{E}h(S_2 + \Delta b(S_2) + \hat{\sigma}(S_2)W) \\ &= \mathbb{E}[\mathbb{E}h(S_2 + \Delta b(S_2) + \hat{\sigma}(S_2)W) | S_1] \\ &\geq \mathbb{E}[h(\mathbb{E}(S_2|S_1) + \Delta \mathbb{E}(b(S_2)|S_1) + \mathbb{E}(\hat{\sigma}(S_2)|S_1)W)] \\ &= \mathbb{E}[h(S_1 + \Delta b(S_1) + \mathbb{E}(\hat{\sigma}(S_2)|S_1)W)] \end{aligned} \quad (26)$$

Here, the linearity of $b(\cdot)$ implies $\mathbb{E}(b(S_2)|S_1) = b(S_1)$. Note that the function $f(x) = \sqrt{x^2 + 1}$ is convex thanks to

$$f''(x) = \frac{2}{(x^2 + 1)\sqrt{x^2 + 1}} > 0.$$

Similarly, $\sigma(\cdot)$ is convex. Using conditional Jensen's inequality again gives

$$\varpi(S_1) := \mathbb{E}(\hat{\sigma}(S_2)|S_1) \geq \hat{\sigma}(\mathbb{E}(S_2|S_1)) = \hat{\sigma}(S_1). \quad (27)$$

Due to

$$S_1 + \Delta b(S_1) + \mathbb{E}(\hat{\sigma}(S_2)|S_1)W \sim N(\mu, \varpi^2), \quad S_1 + \Delta b(S_1) + \hat{\sigma}(S_1)W \sim N(\mu, \hat{\sigma}^2)$$

with $\mu = \mathbb{E}(S_1 + \Delta b(S_1))$, by Theorem 3.4.7 in Müller and Stoyan [2002], (27) implies that

$$\mathbb{E}[h(S_1 + \Delta b(S_1) + \mathbb{E}(\hat{\sigma}(S_2)|S_1)W)] \geq \mathbb{E}[h(S_1 + \Delta b(S_1) + \hat{\sigma}(S_1)W)] = \mathbb{E}h(\mathcal{A}S_1).$$

Combined with (26) we have proved the convex-ordering property (25).

By the Markov property of the Euler-Maruyama approximation we have

$$\mathcal{G}_K(t, x) = \mathbb{E}[g(\mathcal{A}^{K-1}x)].$$

Let z be a Bernoulli random variable which takes the value $z_1 \in \mathbb{R}$ with probability $p \in (0, 1)$ and the value $z_2 \in \mathbb{R}$ with probability $1 - p$. Then $\mathbb{E}(Z) = pz_1 + (1 - p)z_2$. Then we have

$$h(\mathbb{E}(Z)) = h(pz_1 + (1 - p)z_2) \leq ph(z_1) + (1 - p)h(z_2) = \mathbb{E}h(Z).$$

Using the convex-ordering property (25) of the operator \mathcal{A} we obtain

$$\mathcal{G}_K(t, pz_1 + (1 - p)z_2) = \mathcal{G}_K(t, \mathbb{E}(Z)) = \mathbb{E}[g(\mathcal{A}^{K-1}\mathbb{E}(Z))] \leq \mathbb{E}[g(\mathcal{A}^{K-1}Z)] = \mathcal{G}_K(t, Z) \quad (28)$$

due to g is convex. Take expectation on both sides of (28) gives

$$\mathcal{G}_K(t, pz_1 + (1 - p)z_2) \leq \mathbb{E}[\mathcal{G}_K(t, Z)] = p\mathcal{G}_K(t, z_1) + (1 - p)\mathcal{G}_K(t, z_2),$$

which means $\mathcal{G}_K(t, \cdot)$ is convex. The approximation property (24) implies the convexity of $\mathcal{G}(t, \cdot)$. \square

Proof of Lemma 3.3. Since the solution to (7) is a polynomial process (see example 3.6 in Cuchiero et al. [2012]), from Theorem 3.1 in Filipović and Larsson [2016] it implies

$$\mathcal{G}_i(t, Z_t^i) = \mathbb{E}[g(\hat{Z}_T^i) | \hat{Z}_t^i = Z_t^i] = \exp\{(T-t)G\}P(Z_t^i),$$

where

$$G = \begin{pmatrix} 0 & g_0 & 2 \times 1g_1 & 0 & \cdots & 0 \\ 0 & g_2 & 2g_0 & 3 \times 2g_1 & 0 & \vdots \\ 0 & 0 & 2(g_2 + g_3) & 3g_0 & \ddots & 0 \\ 0 & 0 & 0 & 3(g_2 + 2g_3) & \ddots & p(p-1)g_1 \\ \vdots & & & 0 & \ddots & pg_0 \\ 0 & \cdots & & & 0 & p(g_2 + (p-1)g_3) \end{pmatrix}$$

with

$$g_0 = \theta_i \mu_i, \quad g_1 = g_3 = \theta_i a_i, \quad g_2 = -\theta_i,$$

and $P(Z_t^i) = (0, 1, Z_t^i, (Z_t^i)^2, \dots, (Z_t^i)^p)^\top$. Then there is a constant C_T that depends on T such that

$$|\mathcal{G}_i(t, Z_t^i)| \leq C_T(1 + |Z_t^i|^p).$$

Let τ_n be a localizing sequence for $\mathcal{G}(t, y_t)$. Then we have

$$|\mathcal{G}_i(t \wedge \tau_n, Z_{t \wedge \tau_n}^i)| \leq C_T(1 + |Z_{t \wedge \tau_n}^i|^p),$$

which implies

$$|\mathcal{G}_i(t \wedge \tau_n, Z_{t \wedge \tau_n}^i)|^2 \leq C_T(1 + |Z_{t \wedge \tau_n}^i|^{2p}). \quad (29)$$

Taking \mathcal{F}_0 -condition on both sides of (29) gives

$$\begin{aligned} \mathbb{E} \{ |\mathcal{G}_i(t \wedge \tau_n, Z_{t \wedge \tau_n}^i)|^2 \} &\leq C_T (1 + \mathbb{E} |Z_{t \wedge \tau_n}^i|^{2p}) \\ &\leq C_T \left(1 + \mathbb{E} \left[\sup_n |Z_{t \wedge \tau_n}^i|^{2p} \right] \right) \\ &\leq C_T e^{CT}. \end{aligned}$$

Here, the last inequality holds based on Lemma 2.17 in Cuchiero et al. [2012]. Thus, we complete the proof of this lemma. \square

A.3 Lower bound

Let

$$M(x) := \frac{x^\top A^\top A x}{|x|^2}, \quad x \in \mathbb{R}^d \setminus \{0\}$$

denote the Rayleigh-quotient of $A^\top A$. From Chapter 1 in [Horn and Johnson, 2012] we have that the range of $M(x)$ is equal to the line segment $[\lambda_d^2, \lambda_1^2]$, i.e.,

$$\{M(x) : x \in \mathbb{R}^d \setminus \{0\}\} = [\lambda_d^2, \lambda_1^2] \quad (30)$$

Evaluating the condition (19), we have

$$\begin{aligned} &\frac{(1 + |x|^2) [2x^\top F(x)]}{|x|^4} \\ &= \frac{(1 + |x|^2) \left\{ -2\gamma x^\top \left[\frac{1}{n} A^\top (Ax - b) + \delta x \right] \right\}}{|x|^4} \\ &= \frac{(1 + |x|^2) \left[-2\gamma x^\top \left(\frac{1}{n} A^\top A + \delta I_d \right) x + 2\frac{\gamma}{n} x^\top A^\top b \right]}{|x|^4} \\ &= -\frac{2\gamma x^\top \left(\frac{1}{n} A^\top A + \delta I_d \right) x}{|x|^4} - \frac{2\gamma x^\top \left(\frac{1}{n} A^\top A + \delta I_d \right) x}{|x|^2} + \frac{2\frac{\gamma}{n} (1 + |x|^2) x^\top A^\top b}{|x|^4} \end{aligned}$$

and

$$\begin{aligned}
& \frac{(1 + |x|^2)|G(x)|^2 - (2 - \rho)|x^T G(x)|^2}{|x|^4} \\
&= \frac{(1 + |x|^2) \left[\frac{\gamma^2}{n^2 B} |\sqrt{\|Ax - b\|^2 A^T A}|^2 \right] - (2 - \rho) \frac{\gamma^2}{n^2 B} |x^T \sqrt{\|Ax - b\|^2 A^T A}|^2}{|x|^4} \\
&= \frac{\frac{\gamma^2}{n^2} (1 + |x|^2) \|Ax - b\|^2 |\sqrt{A^T A}|^2 - (2 - \rho) \frac{\gamma^2}{n^2} \|Ax - b\|^2 |x^T \sqrt{A^T A}|^2}{|x|^4} \\
&= \frac{\frac{\gamma^2}{n^2 B} \|Ax - b\|^2 |\sqrt{A^T A}|^2}{|x|^4} + \frac{\frac{\gamma^2}{n^2 B} \|Ax - b\|^2 |\sqrt{A^T A}|^2}{|x|^2} \\
&\quad - \frac{(2 - \rho) \frac{\gamma^2}{n^2 B} \|Ax - b\|^2 \frac{x^T A^T Ax}{|x|^2}}{|x|^2}.
\end{aligned}$$

With $|\sqrt{A^T A}|^2 = \text{tr}(A^T A)$ and the positive constant ρ given below, we obtain

$$\begin{aligned}
& \limsup_{|x| \rightarrow \infty} \frac{(1 + |x|^2) [2x^T F(x) + |G(x)|^2] - (2 - \rho)|x^T G(x)|^2}{|x|^4} \\
&= \limsup_{|x| \rightarrow \infty} \left[-\frac{2\gamma x^T (\frac{1}{n} A^T A + \delta I_d) x}{|x|^2} + \frac{\frac{\gamma^2}{n^2 B} \|Ax - b\|^2 |\sqrt{A^T A}|^2}{|x|^2} + \right. \\
&\quad \left. + \frac{(2 - \rho) \frac{\gamma^2}{n^2 B} \|Ax - b\|^2 \frac{x^T A^T Ax}{|x|^2}}{|x|^2} \right] \tag{31} \\
&= -\frac{\gamma^2}{n^2 B} \liminf_{|x| \rightarrow \infty} \left[\frac{2nB(M(x) + n\delta)}{\gamma} - \text{tr}(A^T A)M(x) + (2 - \rho)M(x)^2 \right] = \\
&= -\frac{\gamma^2}{n^2 B} \inf_{m \in [\lambda_d^2, \lambda_1^2]} q(m, \rho),
\end{aligned}$$

where

$$q(m, \rho) = \frac{2nB(m + n\delta)}{\gamma} - \text{tr}(A^T A)m + (2 - \rho)m^2. \tag{32}$$

Set

$$\vartheta := 2 + \frac{2nB(\lambda_1^2 + n\delta)}{\gamma \lambda_1^4} - \frac{\sum_{i=1}^d \lambda_i^2}{\lambda_1^2}.$$

Note that due to the assumption $\gamma < \bar{\gamma}$ we have $\vartheta > 2$. We claim that

$$\inf_{m \in [\lambda_d^2, \lambda_1^2]} q(m, \rho) > q(\lambda_1^2, \theta) = 0 \tag{33}$$

for all $\rho \in [2, \vartheta)$. First, note that $m \mapsto q(m, \rho)$ is concave for any $\rho \in [2, \vartheta)$, such that its minimum must be attained at one of the boundary values $m \in \{\lambda_d^2, \lambda_1^2\}$. Second, note that $\rho \mapsto q(m, \rho)$ is strictly decreasing for any $m \in (0, \infty)$, such that for (33) it is sufficient to show

$$q(\lambda_d^2, \theta) \geq q(\lambda_1^2, \theta) = 0. \tag{34}$$

Using the assumption $\gamma < \bar{\gamma}$ we obtain

$$\begin{aligned}
q(\lambda_d^2, \theta) &= \frac{2nB}{\gamma} (\lambda_d^2 + n\delta) - \text{tr}(A^T A)\lambda_d^2 + \frac{2nB}{\gamma} (\lambda_1^2 + n\delta) \frac{\lambda_d^4}{\lambda_1^4} - \text{tr}(A^T A) \frac{\lambda_d^4}{\lambda_1^2} \geq \\
&\geq \text{tr}(A^T A) \left(\frac{(\lambda_d^2 + n\delta)}{(\lambda_1^2 + n\delta)} \lambda_1^2 - \lambda_d^2 \right).
\end{aligned}$$

For $\delta = 0$ the right hand side vanishes and (34) is shown. Differentiation shows that the right hand side is increasing in δ , such that (34) holds for all $\delta \geq 0$. Altogether, we have shown that the right hand side of (31) is strictly negative. Thus,

the SDE (18) satisfies the Assumption 5.1 in Li et al. [2019]. Based on Theorem 5.2 in Li et al. [2019], the solution X_t of the SDE (18) satisfies

$$\sup_{0 \leq t < \infty} \mathbb{E}|X_t|^\rho \leq C$$

for all $\rho \in [2, \vartheta)$. Therefore, the lower bound, denoted by η_* , for the asymptotic tail-index of X_t is

$$\eta_* = \vartheta = 1 + \frac{2nB(\lambda_1^2 + n\delta)}{\gamma\lambda_1^4} - \frac{\sum_{i=2}^d \lambda_i^2}{\lambda_1^2}.$$